






RESEARCH ARTICLE | AUGUST 30 2024

XPS study of electroless NiP coating on iron substrate

Special Collection: [Materials for Energy and the Environment](#)

Deborah Biggio  ; Bernhard Elsener  ; Marzia Fantauzzi  ; Antonella Rossi  



Surf. Sci. Spectra 31, 024003 (2024)

<https://doi.org/10.1116/6.0003733>



XPS study of electroless NiP coating on iron substrate

Cite as: Surf. Sci. Spectra 31, 024003 (2024); doi: 10.1116/6.0003733

Submitted: 3 May 2024 · Accepted: 13 August 2024 ·

Published Online: 30 August 2024



Deborah Biggio, Bernhard Elsener, Marzia Fantauzzi, and Antonella Rossi^{a)}

AFFILIATIONS

Dipartimento di Scienze Chimiche e Geologiche, Università di Cagliari, Cagliari 09042, Italy

Note: This paper is part of the 2024 Special Topic Collection on Materials for Energy and the Environment.

^{a)} Author to whom correspondence should be addressed: rossi@unica.it

ABSTRACT

X-ray photoelectron spectroscopy and x-ray-induced Auger electron spectroscopy analyses were performed to characterize NiP coating on the iron substrate. This electroless coating is commonly used for its outstanding corrosion resistance, but it is currently of interest as a hydrogen permeation barrier (HPB) for green hydrogen storage and transportation; thus, NiP coatings are relevant for energy and for the environment.

Key words: XPS, XAES, HPB coating, clean hydrogen storage

© 2024 Author(s). All article content, except where otherwise noted, is licensed under a Creative Commons Attribution (CC BY) license (<https://creativecommons.org/licenses/by/4.0/>). <https://doi.org/10.1116/6.0003733>

Accession #: 01963

Technique: XPS and XAES

Specimen: Electroless NiP coating (10 μm) on technical iron substrate

Instrument: Thermo Scientific Theta Probe

Major Elements in Spectra: Ni and P

Minor Elements in Spectra: C and O

Published Spectra: 7

Spectral Category: Comparison

INTRODUCTION

Electroless NiP coatings (10 μm thick) are deposited on iron to improve corrosion resistance (Refs. 1–4). Their functional property as a hydrogen permeation barrier is also being investigated (Refs. 5–7). This work uses x-ray photoelectron spectroscopy (XPS) and x-ray-induced Auger electron spectroscopy (XAES) to characterize the NiP surface.

SPECIMEN DESCRIPTION (ACCESSION # 01963)

Specimen: Electroless NiP coating 10 μm thick on technical-grade iron substrate.

CAS Registry #: Unknown

Specimen Characteristics: Homogeneous; solid; amorphous; conductor; inorganic compound; and coating

Chemical Name: NiP alloys

Source: Galvanic AG, Wädenswil (Switzerland)

Composition: Ni and P

Form: NiP coating on technical-grade iron substrate (sample size 2 × 2 cm²)

Structure: X-ray diffraction provided evidence that the sample is amorphous; atomic force microscopy (AFM) showed the presence of nanocrystallites (Ref. 4).

History and Significance: Electroless NiP coatings were deposited from a commercial nickel hypophosphite bath at pH 4.8 and 88 °C (Galvanic, Wädenswil, CH). The substrate was a technical-grade iron. Before deposition, the substrate was mechanically polished using Struers SiC 4000 abrasive paper, and hydrochloric acid solution was used as an acid pickling bath. A nickel coating about 1 μm thick was deposited on an iron substrate for the subsequent NiP deposition. Bath formulation was chosen to obtain a phosphorus concentration in the alloy of 18–24 at. % (Refs. 1–4).

As Received Condition: The “as received” NiP sample exhibits hemispherical growth features by AFM. The crystallite size is 1.2 nm, typical for nano-crystalline electroless deposited coatings (Ref. 4).

30 August 2024 13:32:41

Analyzed Region: Center of the sample

Ex Situ Preparation/Mounting: The surface of NiP alloy deposited on iron were mechanically ground using Struers SiC 2400 and 4000-mesh papers; the lubricant was bi-distilled water [1.5 (0.1) $\mu\text{S}/\text{cm}$]. Polishing of NiP surfaces was performed using 3 and $\frac{1}{4}$ μm diamond spray on a velvet (DP-Nap) in the presence of EtOH as lubricant.

In Situ Preparation: None

Charge Control: No charge control

Temp. During Analysis: 300 K

Pressure During Analysis: $< 1 \times 10^{-7}$ Pa

Preanalysis Beam Exposure: 0 s

INSTRUMENT DESCRIPTION

Manufacturer and Model: Thermo Scientific Theta Probe

Analyzer Type: Spherical sector

Detector: Multichannel plate

Number of Detector Elements: 128

INSTRUMENT PARAMETERS COMMON TO ALL SPECTRA

Spectrometer

Analyzer Mode: Constant pass energy

Throughput ($T = E^N$): The energy dependence can be determined

by using the following equation: $\frac{A}{E_p} = \left(\frac{a^2}{(a^2 + R^2)}\right)^b$, where a and b

are constants, E_p is the pass energy, A is the peak area, and R is the retard ratio equal to E/E_p , where E is the photoelectron kinetic energy. Three spectral regions [Cu 2p (925–940 eV), Cu 3p (68–82 eV), and Cu $L_{3,4,5}M_{4,5}$ (561–577 eV)] are recorded on a sputter cleaned copper sample at different pass energies (10, 20, 50, 100, 125, 150, 200, 300, and 400 eV). The values of a and b are then determined; they were found to be equal to 26.66 and 1.11, respectively, by a linear least square fit of the data applying the equation described above (Ref. 8).

Excitation Source Window: None

Excitation Source: Al K_{α} monochromatic

Source Energy: 1486.6 eV

Source Strength: 100 W

Source Beam Size: Nominal spot size: $400 \times 400 \mu\text{m}^2$ —spot size measured by analyzing Au/Si fresh cleaved sample using line scan measurement resulted to be equal to $355.8 \times 219.2 \mu\text{m}^2$

Signal Mode: Single channel direct

Geometry

Incident Angle: 30°

Source-to-Analyzer Angle: 67.38°

Emission Angle: 53°

Specimen Azimuthal Angle: 70°

Acceptance Angle from Analyzer Axis: 60°

Analyzer Angular Acceptance Width: $30^\circ \times 30^\circ$

Ion Gun

Manufacturer and Model: Thermo Scientific EX05

Energy: 3000 eV

Current: 0.002 mA

Current Measurement Method: Biased stage

Sputtering Species and Charge: Ar^+

Spot Size (unrastered): $200 \mu\text{m}$

Raster Size: $3000 \times 3000 \mu\text{m}^2$

Incident Angle: 45.00°

Polar Angle: 58.43°

Azimuthal Angle: 100°

Comment: None

DATA ANALYSIS METHOD

Energy Scale Correction: Plotted NiP binding energies are corrected by setting the C 1s peak to 285.0 eV (Refs. 9–11).

Recommended Energy Scale Shift: All binding energy values were corrected by setting the C 1s at 285.0 eV using a shift of -0.24 eV.

Peak Shape and Background Method: Shirley-Sherwood background subtraction, line shape: mixed product of Gaussian/Lorentzian (GLP) functions.

Quantitation Method: The quantitative composition might be calculated assuming the sample homogeneity from the experimental areas corrected for the relative sensitivity factors that consider: the photoelectric cross sections, σ (Ref. 12) the asymmetry parameter (Ref. 13) and the intensity analyzer response [see section Throughput ($T = E^N$)]. Inelastic mean free path was calculated according to Ref. 14. In this work, the composition is not given because the assumption of homogeneity is not fulfilled being this is a multilayer material.

ACKNOWLEDGMENTS

Giovanni Emanuele Porcedda of University of Cagliari is acknowledged for the calibration of the Theta Probe spectrometer. The financial support of the European Union NextGenerationEU under the National Recovery and Resilience Plan (NRRP) of Ministero dell'Università e della Ricerca (MUR) (Project code PE0000021, "Network 4 Energy Sustainable Transition," NEST) is acknowledged.

AUTHOR DECLARATIONS

Conflicts of Interest

The authors have no conflicts to disclose.

Author Contributions

Deborah Biggio: Conceptualization (equal); Data curation (lead); Investigation (equal); Methodology (equal); Validation (lead); Writing – original draft (lead); Writing – review & editing (equal). **Bernhard Elsener:** Conceptualization (equal); Investigation (supporting); Methodology (equal); Writing – original draft (supporting); Writing – review & editing (equal). **Marzia Fantauzzi:** Conceptualization (equal); Investigation (supporting); Methodology (equal); Writing – original draft (supporting); Writing – review & editing (equal). **Antonella Rossi:** Conceptualization (equal); Funding acquisition (lead); Investigation

(supporting); Methodology (equal); Project administration (lead); Writing – original draft (supporting); Writing – review & editing (equal).

DATA AVAILABILITY

The data that support the findings of this study are available within the article and its [supplementary material](#).

REFERENCES

- ¹M. A. Scorciapino, M. Fantauzzi, M. Crobu, G. Navarra, B. Elsener, and A. Rossi, *ACS Omega* **2**, 7790 (2017).
- ²B. Elsener, M. Crobu, M. A. Scorciapino, and A. Rossi, *J. Appl. Electrochem.* **38**, 1053 (2008).
- ³B. Elsener, D. Atzei, A. Krolikowski, and A. Rossi, *Surf. Interface Anal.* **40**, 919 (2008).
- ⁴M. Crobu, A. Scorciapino, B. Elsener, and A. Rossi, *Electrochim. Acta* **53**, 3364 (2008).
- ⁵S. Samanta, C. Singh, A. Banerjee, K. Mondal, M. Dutta, and S. B. Singh, *Surf. Coat. Technol.* **403**, 126356 (2020).
- ⁶E. A. Esfahani, A. Morina, B. Han, I. Nedelcu, M. C. P. Van Eijk, and A. Neville, *Tribol. Int.* **113**, 433 (2017).
- ⁷M. Hino, Y. Doi, R. Kuwano, Y. Oda, and K. Horikawa, *Mater. Trans.* **62**, 75 (2021).
- ⁸R. Heuberger, A. Rossi, and N. D. Spencer, *Tribol. Lett.* **28**, 209 (2007).
- ⁹M. P. Seah, *Surf. Interface Anal.* **31**, 721 (2001).
- ¹⁰L. H. Grey, H.-Y. Nie, and M. C. Biesinger, *Appl. Surf. Sci.* **653**, 159319 (2024).
- ¹¹U. Gelius, P. F. Hedén, J. Hedman, B. J. Lindberg, R. Manne, R. Nordberg, C. Nordling, and K. Siegbahn, *Phys. Scr.* **2**, 70 (1970).
- ¹²J. H. Scofield, *J. Electron Spectrosc. Relat. Phenom.* **8**, 129 (1976).
- ¹³R. F. Reilman, A. Msezane, and S. T. Manson, *J. Electron Spectrosc. Relat. Phenom.* **8**, 389 (1976).
- ¹⁴M. P. Seah and W. A. Dench, *Surf. Interface Anal.* **1**, 2 (1979).
- ¹⁵B. Elsener, D. Atzei, A. Krolikowski, and A. Rossi, *Surf. Interface Anal.* **40**, 919 (2008).
- ¹⁶M. C. Biesinger, L. W. M. Lau, A. R. Gerson, and R. S. C. Smart, *Phys. Chem. Chem. Phys.* **14**, 2434 (2012).
- ¹⁷H. W. Nesbitt, D. Legrand, and G. M. Bancroft, *Phys. Chem. Miner.* **27**, 357 (2000).
- ¹⁸G. Pagot, M. Benedet, C. Maccato, D. Barreca, and V. Di Noto, *Surf. Sci. Spectra* **30**, 024028 (2023).
- ¹⁹P. M. A. Sherwood, *Surf. Sci. Spectra* **9**, 62 (2002).
- ²⁰J. Kojnok, A. Szasz, W. Krasser, G. Mark, V. S. Stepanjuk, and A. A. Katsnelson, *J. Phys.: Condens. Matter* **4**, 2487 (1992).

SPECTRAL FEATURES TABLE

Spectrum ID #	Element/ Transition	Peak Energy (eV)	Peak Width FWHM (eV)	Peak Area (eV × counts/s)	Sensitivity Factor	Concentration ^a (at. %)	Peak Assignment
01963-02 ^b	Ni 2p _{3/2} 1	852.6	1.3	74 516	23.99	...	Ni of NiP alloy
01963-02 ^b	Ni 2p _{3/2} 2	856.1	1.4	16 422	23.99	...	Ni phosphate
01963-02 ^b	Ni 2p _{3/2} 3,4	859–864	Ni satellites of NiP/Ni phosphate
01963-02 ^b	Ni 2p _{1/2} 5	869.8	NiP alloy
01963-02 ^b	Ni 2p _{1/2} 6	873.3	Ni phosphates
01963-02 ^b	Ni 2p _{1/2} 7,8	878–884	Ni satellites of NiP/Ni phosphate
01963-03 ^c	Ni LMM 1	846.3	Ni L ₃ M _{4,5} M _{4,5}
01963-03 ^c	Ni LMM 2	863.5	Ni L ₂ M _{4,5} M _{4,5}
01963-04 ^d	P 2p _{3/2} 1	129.5	1.0	2 623	2.26	...	Phosphorus—NiP alloy
01963-04 ^d	P 2p _{3/2} 2	131.5	1.4	646	2.26	...	Elemental phosphorus
01963-04 ^d	P 2p _{3/2} 3	133.1	1.4	889	2.26	...	Phosphorus—Ni phosphate
01963-05	O 1s 1	531.3	1.9	25 755	5.85	...	Oxygen—Ni phosphate
01963-05	O 1s 2	533.4	1.9	533	5.85	...	Adsorbed water
01963-06	C 1s 1	285.0	1.4	7 117	1.89	...	Surface contamination
01963-06	C 1s 2	286.7	1.4	839	1.89	...	C—O
01963-06	C 1s 3	288.6	1.4	908	1.89	...	C=O
01963-07	Ni 3d	852.6

^aThe composition is not given because the assumption of homogeneity is not fulfilled since this is a multilayer material. Interested readers might refer to the paper by Scoriapino *et al.* (Ref. 1) for a more accurate quantification of the alloy composition for a similar sample.

^bThe attribution of spectral features 1–8 is in the Footnote to Spectrum #01963-02.

^cPeak positions of Auger signals are given in kinetic energy.

^dEach doublet assigned to P 2p_{3/2} and P 2p_{1/2} was fitted constraining the peak area ratio to 2:1 and the binding energy difference to 0.9 eV (Refs. 1–5). The assignment of the spectral features 1–3 is in Footnote to Spectrum #01963-04.

Footnote to Spectrum #01963-02: The NiP alloy, following mechanical polishing, showed a nickel spectral region which includes the contribution of the NiP coating and that of the surface film made of nickel phosphate (Refs. 1–4 and 15). The signals at 852.6 eV (peak #1) and 869.8 eV (peak #5) are due to the spin–orbit coupling components, Ni 2p_{3/2} and Ni 2p_{1/2}, respectively, of the NiP and are together with the satellites. Peaks #2 and #6 at 856.1 and 873.3 eV are assigned to the spin–orbit coupling components of the nickel in the surface phosphate film. The complex structure (peaks #3, #4, #7, and #8) results from the overlap of the coating and the surface layer satellite signals. The distance of the satellites from the main peak was higher than the value reported for pure nickel, but in agreement with the electronic properties of amorphous NiP alloys (Refs. 1–4 and 15). The presence of NiO and Ni(OH)₂ signals that should be located at 853.8 and at about 856 eV, respectively, can be ruled out according to Refs. 16–18.

Footnote to Spectrum #01963-03: the Ni LMM region showed two main peaks (peak #1, KE = 846.3 and peak #2, KE = 853.5) assigned to the Auger transitions Ni L₃M_{4,5}M_{4,5} and Ni L₂M_{4,5}M_{4,5}, respectively. These signals are the convolution of those due to NiP alloy and nickel phosphate (Refs. 15 and 16).

Footnote to Spectrum #01963-04: The P 2p region showed three main signals at 129.5, 131.5, and 133.1 eV. They are assigned to phosphorus in the bulk alloy (peak #1), to the elemental P (peak #2), and to phosphate (peak #3) (Refs. 1–4, 15, and 19).

Footnote to Spectrum #01963-05: The O 1s spectra exhibited an intense peak at 531.3 eV (peak #1) and a shoulder at 533.4 eV (peak #2). These components might be ascribed to the oxygen in nickel phosphates and to the adsorbed water (Ref. 1).

Footnote to Spectrum #01963-06: The C 1s signal was characterized by the presence of three components. The most intense one, located at BE = 285.0 eV, is related to the surface contamination arising from air exposure before the analysis. The shoulder at BE = 286.7 eV is related to the C—O species, whereas the peak at BE = 288.6 eV is assigned to the presence of the C=O, according to Ref. 10.

Footnote to Spectrum #01963-07: The valence band (VB) exhibits limited resolution and provides an averaged density of states of all near-surface atoms. Although discrimination between the local density of states (DOS) attributable to nickel and phosphorus is challenging, Ni 3d states prevail in the valence band region (Refs. 15 and 20). No differences were observed between the VB spectra of metallic Ni and NiP alloys, as reported in the literature (Refs. 15 and 20).

30 August 2024 13:32:41

ANALYZER CALIBRATION TABLE

Spectrum ID #	Element/Transition	Peak Energy (eV)	Peak Width FWHM (eV)	Peak Area (eV × counts)	Sensitivity Factor	Concentration (at. %)	Peak Assignment
...	Au 4f _{7/2}	83.95	1.04	1 91 600	Gold metal
...	Ag 3d _{5/2}	368.26	0.96	1 97 000	Silver metal
...	Cu 2p _{3/2}	932.61	1.24	1 43 000	Copper metal

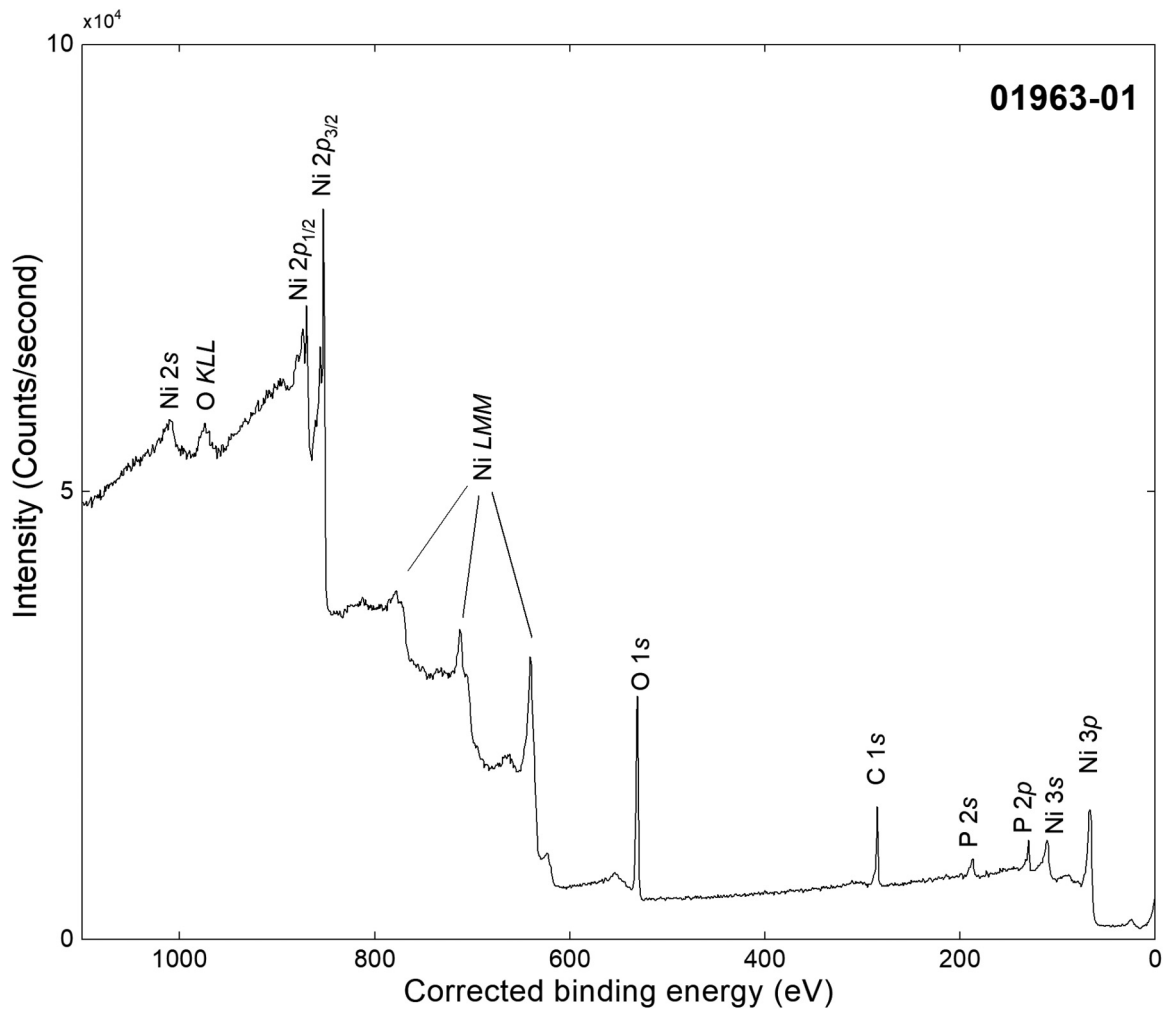
Comment to Analyzer Calibration Table: The spectra were acquired after Ar⁺ etching. Calibration of the binding energy scale was performed following the ISO 15472:2010. Small drifts of the binding energy scale were corrected, and accuracy of ±0.05 eV was determined.

30 August 2024 13:32:41

GUIDE TO FIGURES

Spectrum (Accession) #	Spectral Region	Voltage Shift ^a	Multiplier	Baseline	Comment #
01963-01	Survey	0.24	1	0	...
01963-02	Ni 2p	0.24	1	0	...
01963-03	Ni LMM	0.24	1	0	...
01963-04	P 2p	0.24	1	0	...
01963-05	O 1s	0.24	1	0	...
01963-06	C 1s	0.24	1	0	...
01963-07	Valence band	0.24	1	0	...

^aVoltage shift of the archived (as-measured) spectrum relative to the printed figure. The figure reflects the recommended energy scale correction due to a calibration correction, sample charging, flood gun, or other phenomenon.

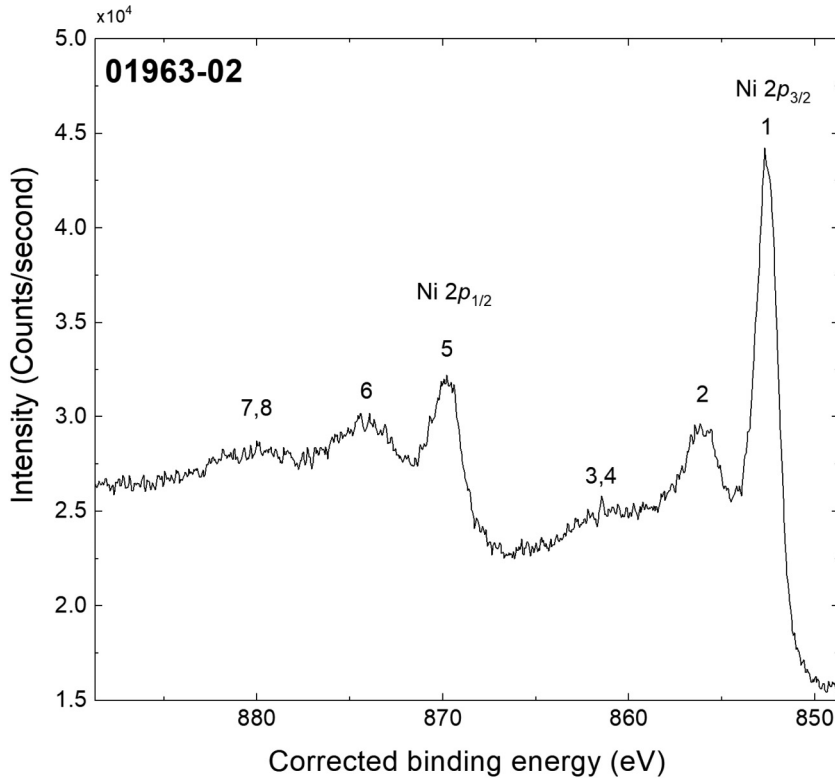


30 August 2024 13:32:41

Accession #:

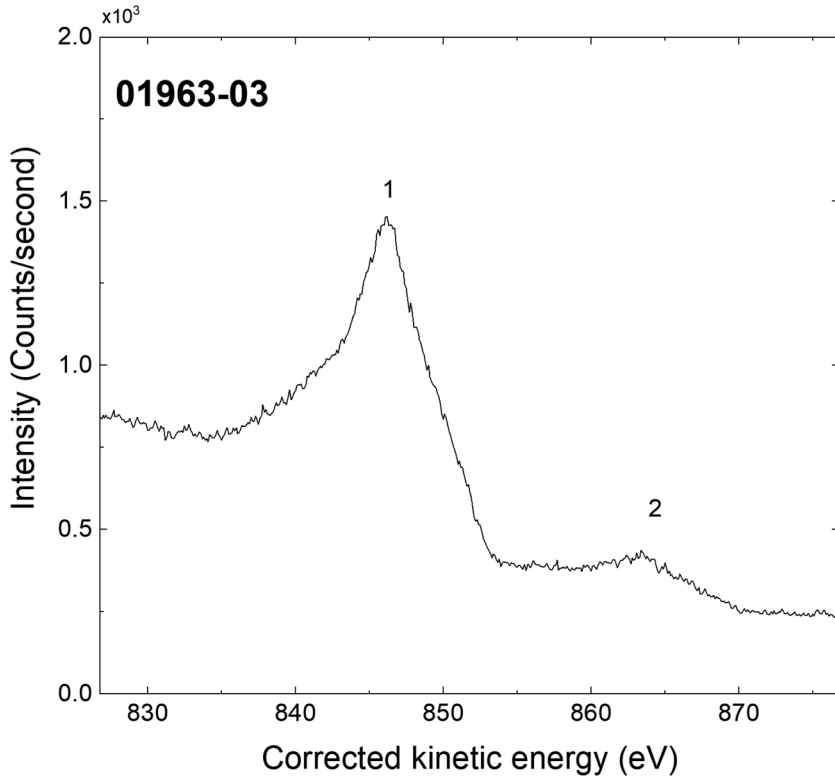
01963-01

■ Specimen:	Mechanically polished electroless NiP on Fe substrate
■ Technique:	XPS
■ Spectral Region:	Survey
Instrument:	Thermo Scientific Theta Probe
Excitation Source:	Al K_{α} monochromatic
Source Energy:	1486.6 eV
Source Strength:	100 W
Source Size:	0.4 × 0.4 mm ²
Analyzer Type:	Spherical sector analyzer
Incident Angle:	30°
Emission Angle:	53°
Analyzer Pass Energy:	200 eV
Analyzer Resolution:	1.5 eV
Total Signal Accumulation Time:	612 s
Total Elapsed Time:	998 s
Number of Scans:	9
Effective Detector Width:	1.0 eV



■ **Accession #:** 01963-02
 ■ **Specimen:** Mechanically polished electroless NiP on Fe substrate
 ■ **Technique:** XPS
 ■ **Spectral Region:** Ni 2p

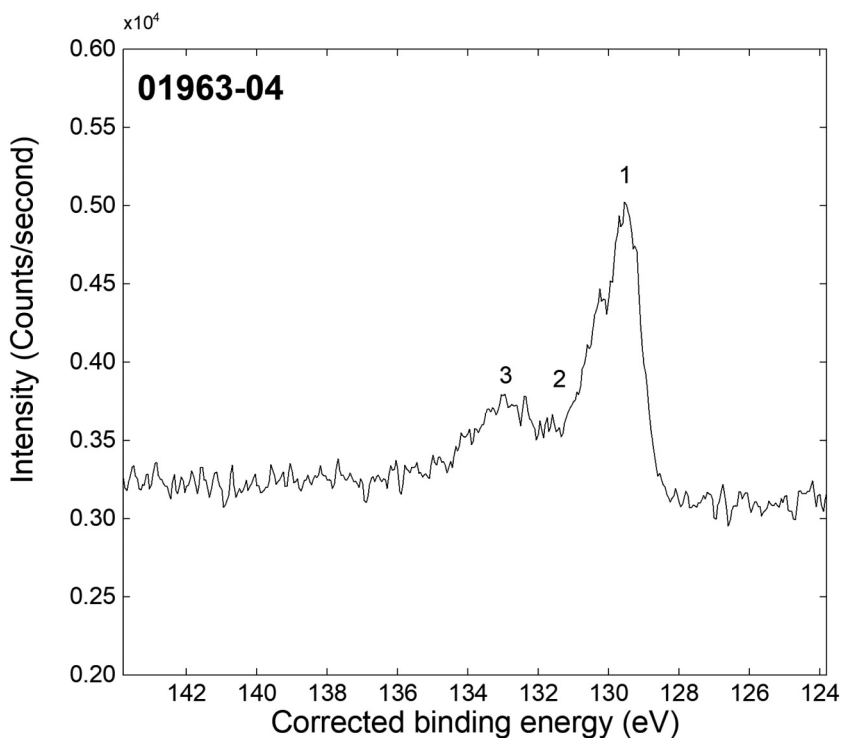
Instrument: Thermo Scientific Theta Probe
 Excitation Source: Al K_{α} monochromatic
 Source Energy: 1486.6 eV
 Source Strength: 100 W
 Source Size: $0.4 \times 0.4 \text{ mm}^2$
 Analyzer Type: Spherical sector
 Incident Angle: 30°
 Emission Angle: 53°
 Analyzer Pass Energy: 100 eV
 Analyzer Resolution: 0.96 eV
 Total Signal Accumulation Time: 126 s
 Total Elapsed Time: 227 s
 Number of Scans: 3
 Effective Detector Width: 0.05 eV



■ **Accession #:** 01963-03
 ■ **Specimen:** Mechanically polished electroless NiP on Fe substrate
 ■ **Technique:** XAES
 ■ **Spectral Region:** Ni LMM

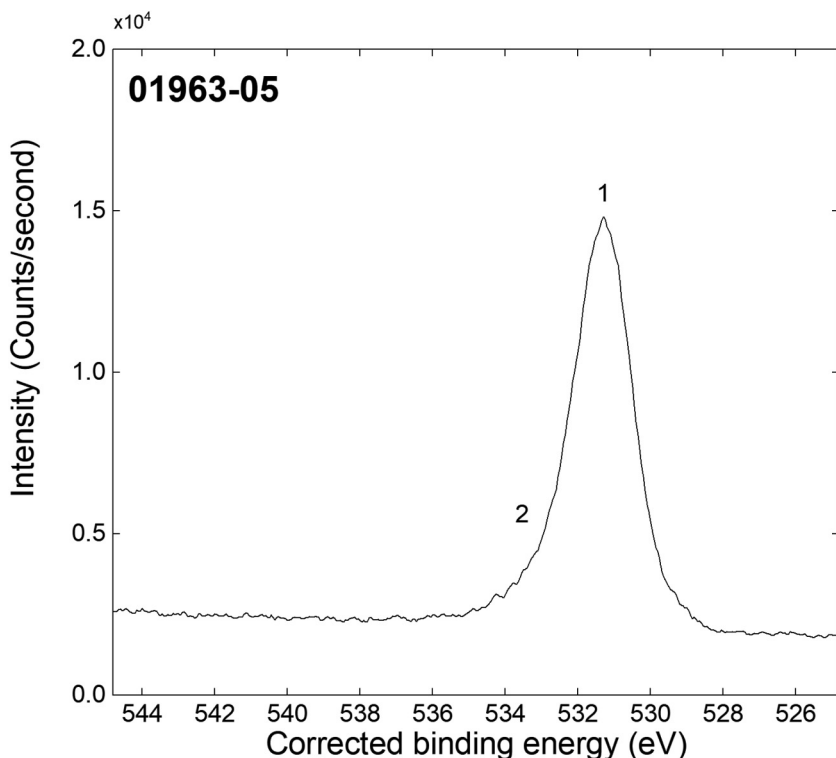
Instrument: Thermo Scientific Theta Probe
 Excitation Source: Al K_{α} monochromatic
 Source Energy: 1486.6 eV
 Source Strength: 100 W
 Source Size: $0.4 \times 0.4 \text{ mm}^2$
 Analyzer Type: Spherical sector
 Incident Angle: 30°
 Emission Angle: 53°
 Analyzer Pass Energy: 100 eV
 Analyzer Resolution: 0.96 eV
 Total Signal Accumulation Time: 225 s
 Total Elapsed Time: 394 s
 Number of Scans: 9
 Effective Detector Width: 0.1 eV

30 August 2024 13:32:41



- **Accession #:** 01963-04
- **Specimen:** Mechanically polished electroless NiP on Fe substrate
- **Technique:** XPS
- **Spectral Region:** P 2p

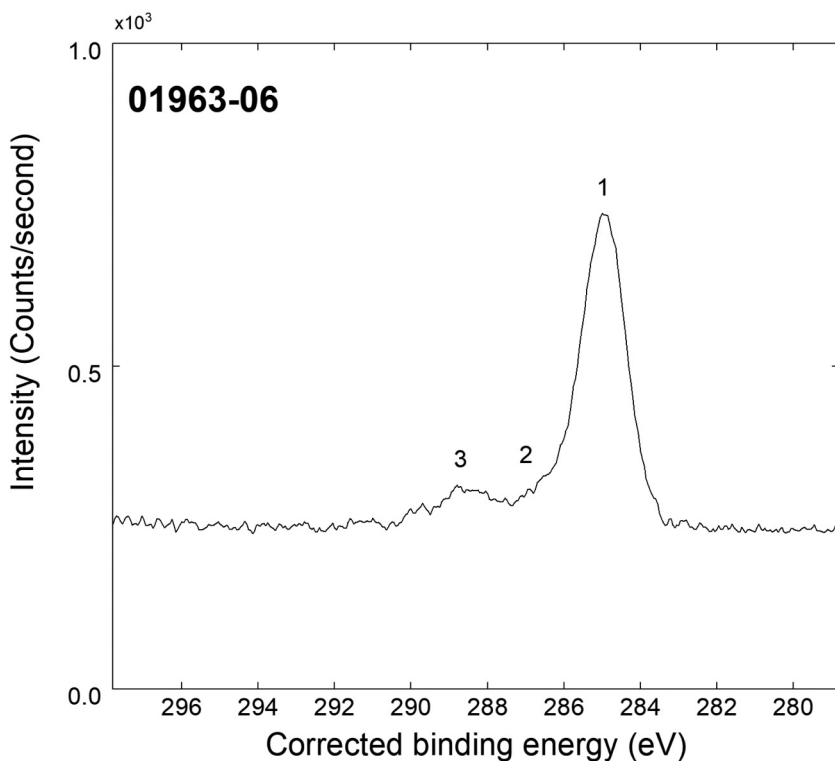
Instrument: Thermo Scientific Theta Probe
 Excitation Source: Al K_{α} monochromatic
 Source Energy: 1486.6 eV
 Source Strength: 100 W
 Source Size: 0.4 × 0.4 mm²
 Analyzer Type: Spherical sector
 Incident Angle: 30°
 Emission Angle: 53°
 Analyzer Pass Energy: 100 eV
 Analyzer Resolution: 0.96 eV
 Total Signal Accumulation Time: 180 s
 Total Elapsed Time: 400 s
 Number of Scans: 9
 Effective Detector Width: 0.05 eV



- **Accession #:** 01963-05
- **Specimen:** Mechanically polished electroless NiP on Fe substrate
- **Technique:** XPS
- **Spectral Region:** O 1s

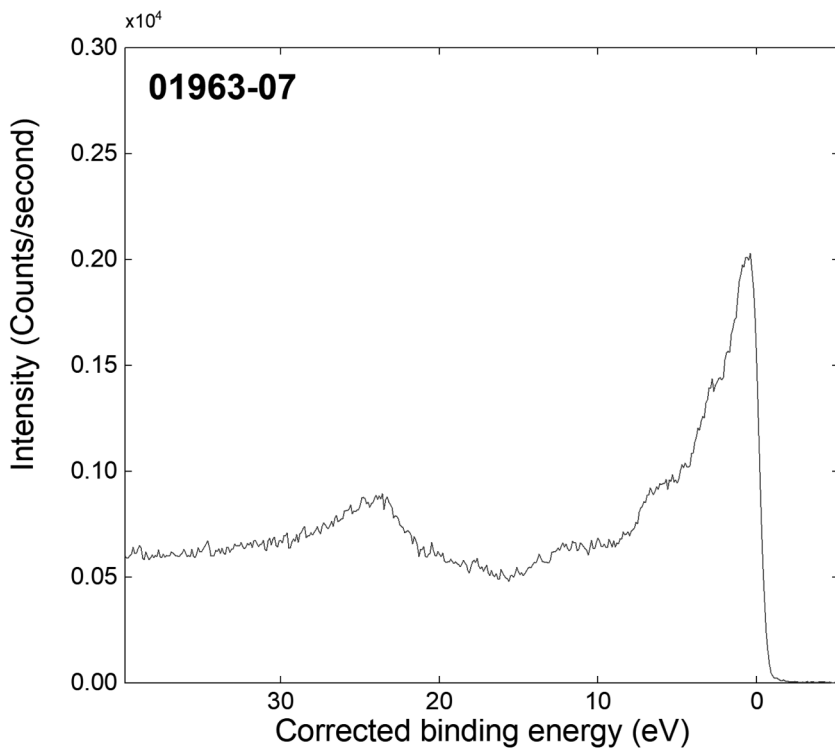
Instrument: Thermo Scientific Theta Probe
 Excitation Source: Al K_{α} monochromatic
 Source Energy: 1486.6 eV
 Source Strength: 100 W
 Source Size: 0.4 × 0.4 mm²
 Analyzer Type: Spherical sector
 Incident Angle: 30°
 Emission Angle: 53°
 Analyzer Pass Energy: 100 eV
 Analyzer Resolution: 0.96 eV
 Total Signal Accumulation Time: 180 s
 Total Elapsed Time: 395 s
 Number of Scans: 9
 Effective Detector Width: 0.05 eV

30 August 2024 13:32:41



- **Accession #:** [01963-06](#)
- **Specimen:** Mechanically polished electroless NiP on Fe substrate
- **Technique:** XPS
- **Spectral Region:** C 1s

Instrument: Thermo Scientific Theta Probe
 Excitation Source: Al K_{α} monochromatic
 Source Energy: 1486.6 eV
 Source Strength: 100 W
 Source Size: $0.4 \times 0.4 \text{ mm}^2$
 Analyzer Type: Spherical sector
 Incident Angle: 30°
 Emission Angle: 53°
 Analyzer Pass Energy: 100 eV
 Analyzer Resolution: 0.96 eV
 Total Signal Accumulation Time: 171 s
 Total Elapsed Time: 381 s
 Number of Scans: 9
 Effective Detector Width: 0.05 eV



- **Accession #:** [01963-07](#)
- **Specimen:** Mechanically polished electroless NiP on Fe substrate
- **Technique:** XPS
- **Spectral Region:** Valence Band

Instrument: Thermo Scientific Theta Probe
 Excitation Source: Al K_{α} monochromatic
 Source Energy: 1486.6 eV
 Source Strength: 100 W
 Source Size: $0.4 \times 0.4 \text{ mm}^2$
 Analyzer Type: Spherical sector
 Incident Angle: 30°
 Emission Angle: 53°
 Analyzer Pass Energy: 100 eV
 Analyzer Resolution: 0.96 eV
 Total Signal Accumulation Time: 608 s
 Total Elapsed Time: 1084 s
 Number of Scans: 27
 Effective Detector Width: 0.05 eV

30 August 2024 13:32:41